

Article

The Use of Machine Learning and Satellite Imagery to Detect Roman Fortified Sites: The Case Study of Blad Talh (Tunisia Section)

Nabil Bachagha ^{1,*}, Abdelrazek Elnashar ² , Moussa Tababi ³, Fatma Souei ⁴ and Wenbin Xu ¹ ¹ The School of Geo-Science and Info-Physics, Central South University, Changsha 410006, China² Department of Natural Resources, Faculty of African Postgraduate Studies, Cairo University, Giza 12613, Egypt³ Faculty of Letters and Humanities of Sousse, University of Sousse, FLSHS-LR, Sousse 13ES11, Tunisia⁴ Department of Computer Science, Hunan University, Changsha 410082, China

* Correspondence: bachaghanabil@csu.edu.cn

Abstract: This study focuses on an ad hoc machine-learning method for locating archaeological sites in arid environments. Pleiades (P1B) were uploaded to the cloud asset of the Google Earth Engine (GEE) environment because they are not yet available on the platform. The average of the SAR data was combined with the P1B image in the selected study area called Blad Talh at Gafsa, which is located in southern Tunisia. This pre-desert region has long been investigated as an important area of Roman civilization (106 BCE). The results show an accurate probability map with an overall accuracy and Kappa coefficient of 0.93 and 0.91, respectively, when validated with field survey data. The results of this research demonstrate, from the perspective of archaeologists, the capability of satellite data and machine learning to discover buried archaeological sites. This work shows that the area presents more archaeological sites, which has major implications for understanding the archaeological significance of the region. Remote sensing combined with machine learning algorithms provides an effective way to augment archaeological surveys and detect new cultural deposits.

Keywords: archaeological; machine learning; Google Earth Engine; remote sensing; fortified sites



Citation: Bachagha, N.; Elnashar, A.; Tababi, M.; Souei, F.; Xu, W. The Use of Machine Learning and Satellite Imagery to Detect Roman Fortified Sites: The Case Study of Blad Talh (Tunisia Section). *Appl. Sci.* **2023**, *13*, 2613. <https://doi.org/10.3390/app13042613>

Academic Editor: Tung-Ching Su

Received: 20 January 2023

Revised: 10 February 2023

Accepted: 12 February 2023

Published: 17 February 2023



Copyright: © 2023 by the authors. Licensee MDPI, Basel, Switzerland. This article is an open access article distributed under the terms and conditions of the Creative Commons Attribution (CC BY) license (<https://creativecommons.org/licenses/by/4.0/>).

1. Introduction

Similar to most research-driven fields, archaeology fundamentally depends on the following two precious and scarce resources: time and money [1]. Archaeologists often travel long distances to reach areas of interest and devote a considerable amount of time to excavations and surveys. Additionally, the discovery of archaeological sites is among the most time-consuming and labour-intensive activities. Archaeologists often use advanced technologies to search for less expensive and faster methodologies for archaeological research. Southern Tunisia is a vast region with difficult access to the investigation area and limited opportunities for in-person data collection. Consequently, land managers spend precious and dwindling resources conducting expensive surveys that result in very few representative samples. One way to address this problem is to develop survey strategies that focus on archaeological potential. Satellite image analysis is a relatively low-cost method with great potential for addressing these needs. The application of remote sensing technology is an effective method for producing relatively complete records of archaeological settlement patterns and human activity at the landscape scale. The literature concerning archaeological remote sensing (RS) has shown that multispectral satellite sensors and airborne LiDAR are particularly useful for addressing survey coverage and positioning issues [2–7]. In many regions worldwide, RS has been used to detect and map archaeological proxy indicators [8–12] by leveraging multisource imagery and spatial pattern analyses. RS technologies enable the discovery of new sites and maps

of ancient remnants and can be used to assist with the digital reconstruction of ancient monuments and their environmental backgrounds. For example, in Mediterranean regions, such as Greece and Croatia, several studies have demonstrated excellent performance using a variety of passive and active remote sensing data (including multispectral imagery, thermal images, and UAV-based LiDAR data) to identify ancient Roman remains [13–17]. Fonte et al. [18] evaluated and debated the use of digital modelling tools in northwestern Iberia to identify and define Roman roads through GIS-based spatial analyses.

In recent years, RS-based progressive archaeological studies have steadily integrated machine-learning algorithms that enable automated feature finding [19]. Most applications of these methods have focused on small-scale feature detection using LiDAR [20–22] or WorldView satellite data [8,23,24]. In the east, Menze and Ur [25] applied a random forest (RF) classifier to a multitemporal collection of ASTER imagery to classify probable anthrosols. In the Cholistan Desert, Hector et al. [19] applied an RF classifier that integrates a multisensor, multitemporal machine learning approach to detecting archaeological mounds, and Abdulmalik et al. [26,27] used an artificial neural network model combined with a geographic information system (GIS) and remote sensing for surface water detection. Other studies have used multiple types of information to identify archaeological remains or threats to archaeological heritage, such as urban sprawl and archaeological looting [28–30]. Combined with machine learning algorithms, remote sensing provides an effective way to expand investigation areas and detect new cultural deposits [31–34]. In particular, the application of this technology allows researchers to (1) investigate remote areas that are not easy to access due to harsh geography and (2) survey vast and complex environments (characterised, for example, by otherwise challenging topography). Platforms, such as Google Earth Engine (GEE) [35], provide a scalable, cloud-based, geospatial retrieval and processing platform, particularly in remote areas with little or almost no ground information. Google Earth Engine is a cloud-based platform that makes it simple to access high-performance computing resources for covering geospatial datasets. Once an algorithm is developed on GEE, users can produce regular data products or deploy interactive applications powered by Google Earth Engine resources. Archaeologists have only recently begun to search for more complex models, drawing on innovative analysis of spatial and statistical computing and machine learning methods [36,37]. To date, these studies are increasing when dealing with the detection of archaeological sites based on high-resolution satellite or drone imagery and in pottery classification [38–40]. Several studies have applied different methods for the identification of buried structures [5,41]. For instance, in arid or desert environments, satellite remote data provides very reliable results that can be used to analyse archaeological sites and their environments. According to previous research, there are more Roman civilisation sites in this area [8], but only a few have been uncovered by remote sensing methods and identified the major distinguishing features of Roman settlements, such as villa and tower walls. In this context, the discovery of archaeological features using machine learning classification algorithms has emerged as one of the most important topics regarding remote sensing; it is an important method to better understand and reconstruct ancient landscapes. Thus far, these topics have mainly been studied by experts, sometimes with the help of automated tools, which results in a very costly and time-consuming process. Therefore, in recent years, many automation methods combining satellite image processing with machine learning models have been developed [19,42–45].

Due to the difficult geography, the investigation of ancient sites in this region is not easy; therefore, machine learning via satellite can play an important role in the detection and documentation of archaeological sites. The aim of this study is to evaluate the potential offered by the combined use of remote sensing data and machine learning to discover fortified sites in arid areas. An innovative aspect of our approach is the combination of very high spatial resolution satellite (PB1) technology with SAR data for better detection and to help obtain enhanced results.

2. Materials and Methods

2.1. Study Area

The study area is positioned in Blad Talh (see Figure 1). The weather is hot, and the average temperature is 19.6 °C; the location receives less than 100 mm of precipitation annually [46,47]. The climate is characterised by extremely irregular rainfall that varies across seasons and within the same season. The alternation of rainy and dry years occurs without a defined pattern, and periods of prolonged drought often occur. The location of Blad Talh (between 34°26'8.18" N and 34°21'36.52" N and between 9°20'3.93" E and 9°30'56.12" E) is shown in Figure 1. It is formed by a series of high plains that are separated by mountains and gradually descend towards the south. Blad Talh has a maximum height of 1165 metres and is characterised by a unique morphology. Blad Talh has been the subject of several studies, mostly geological in nature, that assessed the tectonic and structural formation of two mountain ranges, the Orbita-Bouhedma and Chemsî-Belkhir. Despite its geographical position, located less than 40 km from the Mediterranean and more than 100 km north of the Sahara, Blad Talh is part of pre-Saharan Tunisia, bordered to the north by the Orbita-Bouhedma link, and is classified in the arid bioclimatic stage. This region played an important historical role in the Roman era and was part of the sensitive defence system (Limes) located along the desert border, as attested by the several forts that provided protection [8,46–49]. Many sites that appear to be military structures—forts or towers of various sizes—have been identified at these locations based on their layouts and the methods used to construct them. The study area, Blad Talh, was a region of great importance in Roman times. In a report by Toussaint on the campaign of 1902–1903 [50], we found that the fortification of KSAR GROUECH was especially important. The general assessment of this report leads to the conclusion that the Roman ruins in the region of Blad Talh are very numerous in the plains and much rarer and even less important in the mountainous regions.

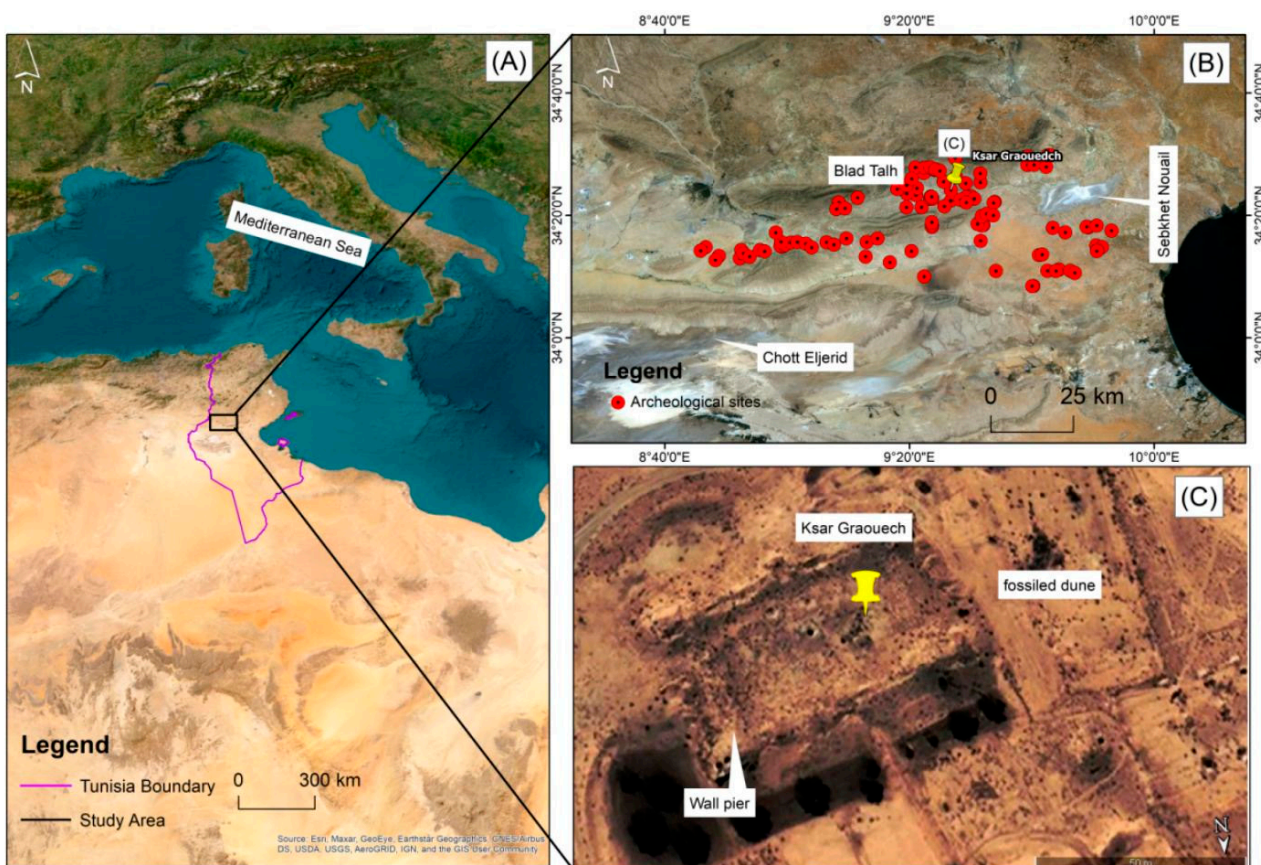


Figure 1. (A) Study area location in Tunisia (North Africa); (B) Archaeological sites in the Roman Fort area; (C) Fort of KSAR GRAOUECH surrounding wall and remains.

2.2. Methodology

The study describes the process of archaeological site detection and the development of an integrated approach that includes remote sensing, a geographic information system, and random forest to achieve these objectives. First, we selected Blad Talh for this research because of the authenticated archaeological remains and the opportunity to gather survey information for this project in November 2021. In total, 101 known archaeological sites are located in Sebkhet Nouail (Figure 1B). Based on a field survey of the entire study area, the archaeological sites in this area were classified. After the field sample collection was carried out by GNSS, satellite imagery was used to locate the archaeological sites at each selected location using ArcGIS based on the actual locations identified by the GNSS instrument. The second step is to use very high resolution (VHR) data to delineate and map study area sites, as well as Sentinel-1 data, which is used as input to help achieve better results. For geometric corrections, these images were imported into the ArcGIS 10.4 package using WGS 84 and UTM zone 32. In the third step, a random forest was applied using a combination of VHR and SAR data in this study, while employing Google Earth Engine as a platform to decrease the computational time and avoid any other barriers. These sensors were a crucial factor in ensuring that the features that would generate values analogous to those of spots in one source were distinguished from the other features. The final step was survey validation and determining archaeological site significance using remote sensing-based archaeological surveys. Remote sensing, machine learning, and GNSS allow us to identify unknown sites and provide new directions for future archaeological research in our study area in the ancient Roman period. The overall methodology is presented in Figure 2, while the specifics of each major section are given in the subsequent sections.

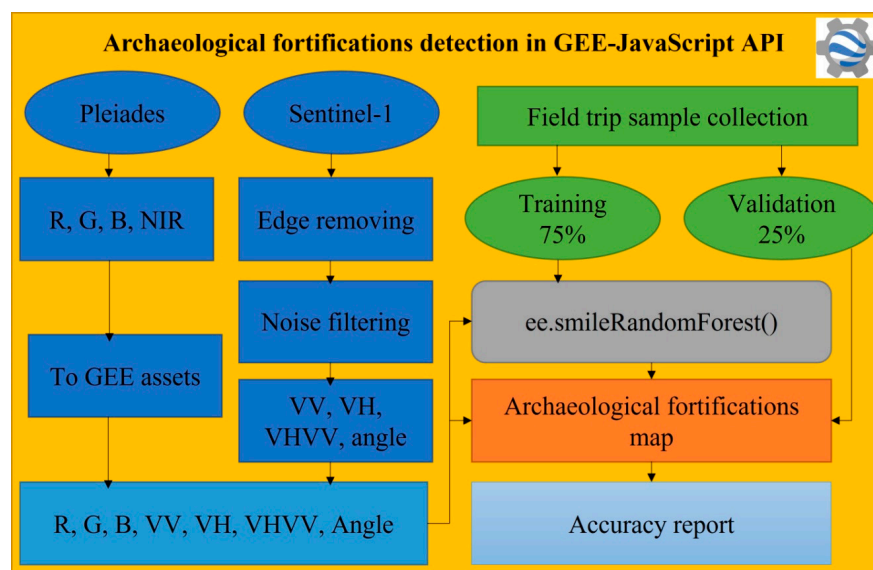


Figure 2. Framework approach.

2.3. Field Investigation Sample Collection

We selected Blad Talh for this research because of the authenticated archaeological remains and the opportunity to gather survey information for this project. The database recaptured from the historic record of the region allowed an overview of the literature review of the Roman period. The GIS integration of the results of these different steps was critical to planning a systematic field survey focused on specific areas of interest, for which the primary results are presented. In November 2021, the search team arrived at the study area of interest. A number of ceramic African sigils were found at these sites. Along these roads, we have classified these sites of interest as being Roman fortified structures based on the ancient remains observed at these sites. By coordinating our findings with GIS, remote sensing, and machine learning, the importance of these new fortifications allowed

speculation regarding their ancient conditions. By confirming our results with remote sensing images and machine learning, we aimed to study the spatial distributions of the archaeological remains and reconstruct the Roman settlement in the region.

2.4. Data Preprocessing

2.4.1. Pleiades

These images were obtained from the Pleiades sensor (P1B) in a strip of the Blad Talh region with the simultaneous acquisition of panchromatic and multispectral information in the Universal Transverse Mercator (UTM) planar projection, Zone 32 N, and WGS 84 datum on 16 July 2021. Of course, the two sets of bands had two different geometric resolutions (Table 1). While the multispectral bands had a ground resolution of 2.14 m, we used 2.14 * 2.14 m/px. The acquisition in the multispectral mode was subdivided into the following four bands of the spectrum: NIR, red, green, and blue. In the first stage of the analysis, P1B images were used to study the archaeological landscape [51] and highlight the most important areas where the cartographic features were determined (boundaries, forts, sites, etc.).

Table 1. Pleiades data from Blad Talh acquired on 16 July 2021.

Band Name	Wavelength (nm)	Spatial Resolution (m)
Blue	430–550	2.14
Green	500–620	2.14
Red	590–710	2.14
Near-infrared	740–940	2.14

2.4.2. Sentinel-1

Sentinel-1 (S1) in the band C imagery contains a 12- or 6-day revisit cycle depending on the availability of images 1A and 1B with 10 m spatial resolution. The analysis presented here selected the interferometric wide swath mode, which is the main operational mode and produces data in single (HH or VV) or double (HH + HV or VV + VH) polarisation in both ascending and descending modes. Each scene available at GEE was preprocessed using the Sentinel-1 Toolbox to (1) remove low-intensity noise and invalid data from scene edges and (2) remove thermal noise [19]. The edge of S1 was omitted using the ‘connected components’ method in GEE, which hides sets of contiguous pixels processed with values less than -25 dB in the VV polarisation [52,53]. The VV and VH noises were filtered using the refined Lee filter [54]. We collected S1 data on 13 and 18 July 2021. In this study, the mean of both images was combined with the Pleiades image. In addition, Sentinel-1 data helped obtain better results. SAR is able to reflect the soil’s roughness, texture, and the different physical conditions of the ground. Another benefit of using SAR is that it has a certain amount of soil penetration in dry sand, which makes it particularly suitable for this specific area.

2.4.3. Processing Environment

The Google Earth Engine (GEE) platform is currently a free answer to the matter of restricted access to processing power [19,35]. GEE is a cloud-based platform that enables a planetary-scale analysis of petabytes of freely obtainable satellite imagery. Combining this large amount of information with the parallel computing strength of Google’s infrastructure facilitates the rapid and easy evaluation of satellite images. GEE parallelises and executes code developed in JavaScript or Python, exploiting Google’s cloud computing infrastructure and allowing work with intensive processes at new scales. This study used GEE for the following three reasons: (1) it is a free platform that has many built-in functions for geospatial analysis and provides quick results without downloading datasets to a local storage system; (2) it has been widely used in several environmental studies [55–57]; and (3) it uses one processing environment and may reduce the uncertainties introduced by various techniques, such as temporal aggregation, resampling (e.g., downscaling and

upsampling), and data reprojection. Notably, the final results from the GEE could be used to create maps (raster.tif) and tables (table.csv) in Google Drive for further processing in the Google Collaboratory (Colab) cloud service [58]. Pleiades bands (blue, green, red, and NIR) were uploaded to the cloud asset of the GEE environment because they are not yet available in the Earth Engine. Thus, the overall framework of the research can be applied to other regions to achieve related aims.

2.4.4. Random Forest Classifier and Accuracy Report

Several artificial intelligence models can be used to process geospatial data when searching for sites in different environments [34,59–62]. The present study aims to detect and map fortified archaeological sites using an integrated method composed of RS data, GIS, field surveys, and a random forest algorithm. The steps of this model followed to classify archaeological sites included categorising the image composite, collecting training data, training the classifier model, and validating the classifier with a separated dataset. We use a selection of 101 archaeological sites linked in Blad Talh's investigation on pre-desert zones as our training ($n = 76$) and confirmation ($n = 25$) sets. Notwithstanding the existence of quality problems in Blad Talh's data, we sort out those sites that might be evidently specified and precisely situated in the high-resolution imagery obtainable in GEE. These matched up with large and well-preserved sites. Polygons were drawn in GEE to outline the areas of the designated sites from which pixel values in the image composite could be extracted for algorithm training. The random forest classification algorithm was applied in this study [56,63,64]. An RF classifier was chosen for the GEE machine-learning implementation. The RF establishes a number of 128 trees on preliminary training samples, but it takes every split in a tree into consideration. For instance, a new subset of predictors is considered randomly in every split when splitting nodes. In addition, the average of the resulting trees helps to evade overfitting and is therefore more stable and reliable than the other decision tree-based classifiers [63,65]. Moreover, RF classifiers can handle a small number of training samples, and it is possible to get the number of votes for each class. These are two advantages that are particularly useful for RS-based archaeology with limited land-use and cover information. In the current GEE algorithm, the RF is combined with trees, which is considered a sufficient value to gain perfect results without unnecessarily increasing the computational cost. The probability mode of the RF was set to evaluate, filter, and refine the results to ameliorate the algorithm's detection potential.

Usually, 75% of the samples are used for the training tree, while the remaining 25% are used for confirmation [63,65]. Herein, the machine-learning process went through three iterations. The original iteration of the algorithm generated pleasant results in that it had the ability to explicitly categorise known sites used as training data and many potential sites by high RF probability values. However, two additional iterations were necessary to adjust the pixels to higher percentages that did not correspond to archaeological sites. RF classifier analysis is a probability domain in bitmap format, where each value records the probability that a given pixel is a "vulnerable site." The RF probability limit for the site values was determined after careful examination of the test data on high-resolution images, which produced a raster map of the clusters ("fortified sites"). A higher threshold resulted in better identification of large, clear sites, but many small pixel clusters corresponding to the small sites covered were lost. Confusion metrics were used to calculate RF accuracy, including the overall accuracy and kappa coefficient. Several researchers demonstrated the perfect application of the GEE platform for training and applied an RF classifier due to its high performance [19,66].

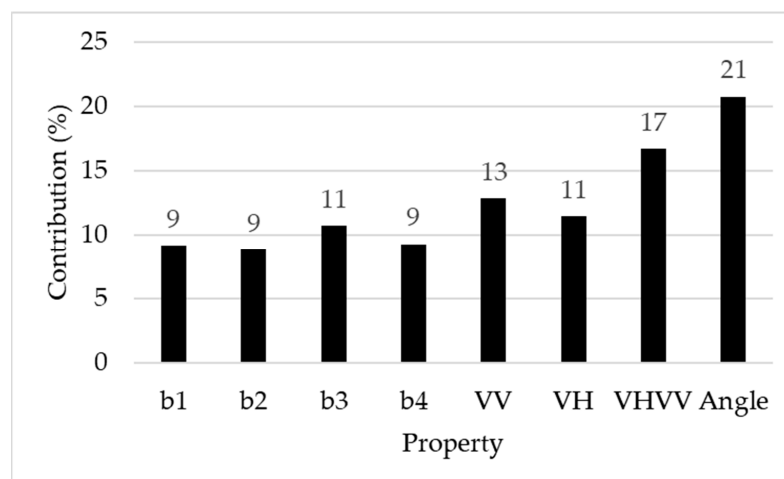
3. Results

Using the proposed methodology, we succeeded in detecting fortified sites that were previously unknown in Blad Talh. The automated detection of fortified sites exhibited high accuracy, equal to that of human detection. The results show that machine learning performed with high accuracy (see Table 2).

Table 2. Classification results of the study area.

Type	Overall Accuracy	Kappa Coefficient
Validation	0.93	0.91

The image combines SAR bands (a single VV and VH and a dual VH–VV band) and P1B bands (b1–b4) (as shown in Figure 3). The high-quality P1B and Sentinel-1 bands are not affected by specific environmental or vision conditions.

**Figure 3.** Feature importance in the classification model.

To the best of our understanding, as of mid-2021, the P1B image received on 16 July 2021 was the most current VHR optical satellite image covering Blad Talh that was accessible online through the GEE. The GEE and machine learning have proven to be applicable instruments for automatically detecting archaeological sites in satellite images. The GEE, machine learning, and remote sensing were highly effective at the site scale and identified pixels of archaeological remains. Furthermore, pixels of fortified structures were successfully detected in Blad Talh, confirming the ability of the GEE to quickly run an analysis on a substantial scale. The discovery and distribution of archaeological sites extended towards the southern part of the Blad Talh area and the surrounding pre-desert towards the east, which was a region that was relatively unreachable in past investigations. Predictably, the allocation of the fortified sites detected by the algorithm was concentrated in the Blad Talh area. Sentinel-1 texture differences between layers were accentuated in the area (see Figure 3).

The algorithm's ability to detect fortified archaeological sites is likely due to polarisation bands and the capacity of the SAR C-band to penetrate soil. Because of vegetation and sand cover, the RF potential produced only some well-illustrated square shapes. The majority of the newly proposed fortified sites presented segmented square shapes or amorphous groups of pixels. It is quite possible that in addition to these five detection sites, there are also remains of sand-covered archaeological sites with low RF probability values. Notably, when high-resolution visible images were used, the algorithm still assisted in identifying small pixels or backscattering. SAR alone showed no significant change in land cover. As a result, SAR alone cannot give enough information to identify archaeological sites. Also, the Pleiades images are not capable of segregating the spectral structures of the sites on their own using an RF classifier. Furthermore, our algorithm was designed to integrate Sentinel-1 and PB1 images for better archaeological discovery, an approach that showed accurate results (see Figure 4). Comparing the results between high-resolution imagery PB1 without SAR images and the virtual absence of sites, their combination for archaeological detection of the known fortified site was used as a validation set (see Figure 4). When possible, the new detection was matched to previous research on past archaeological sites [8,47,67]. The

archaeological sites relative to the existence of sand dunes suggested that many more sites can be covered or located underground in the pre-desert, and thus, the aeolian sediments in southern Tunisia may have played an important role in both the field records of the area and the discernibility of the archaeological ruins. Regions with a large number of sites were located in open mudflats that were distributed throughout the area, while many sites were still relatively covered underground. Five newly detected fortified sites were identified (see Figure 5). The distribution of the archaeological sites extended towards the southern part of the Blad Talh area and the surrounding pre-desert towards the east, which was a region that was relatively unreachable in past investigations. The resulting cluster of high-RF probability pixels showing fortified sites was used to rebuild the regions. Image interpretation was performed using P1B, SAR data, and machine learning. The blend of these data secured enough environmental variability and time to estimate and determine the potential extent of the fortified sites that the algorithm specified. Because of the sand cover, the RF probability yielded only a few well-defined square shapes. Most of the newly proposed sites present fragmentary square shapes and elongated bands of pixels. It is quite possible that in addition to these discovered sites, there are also the remains of archaeological sites covered by sand or shrub vegetation with low RF probability values. It is worth emphasizing that the algorithm helped to identify small groups of site pixels.

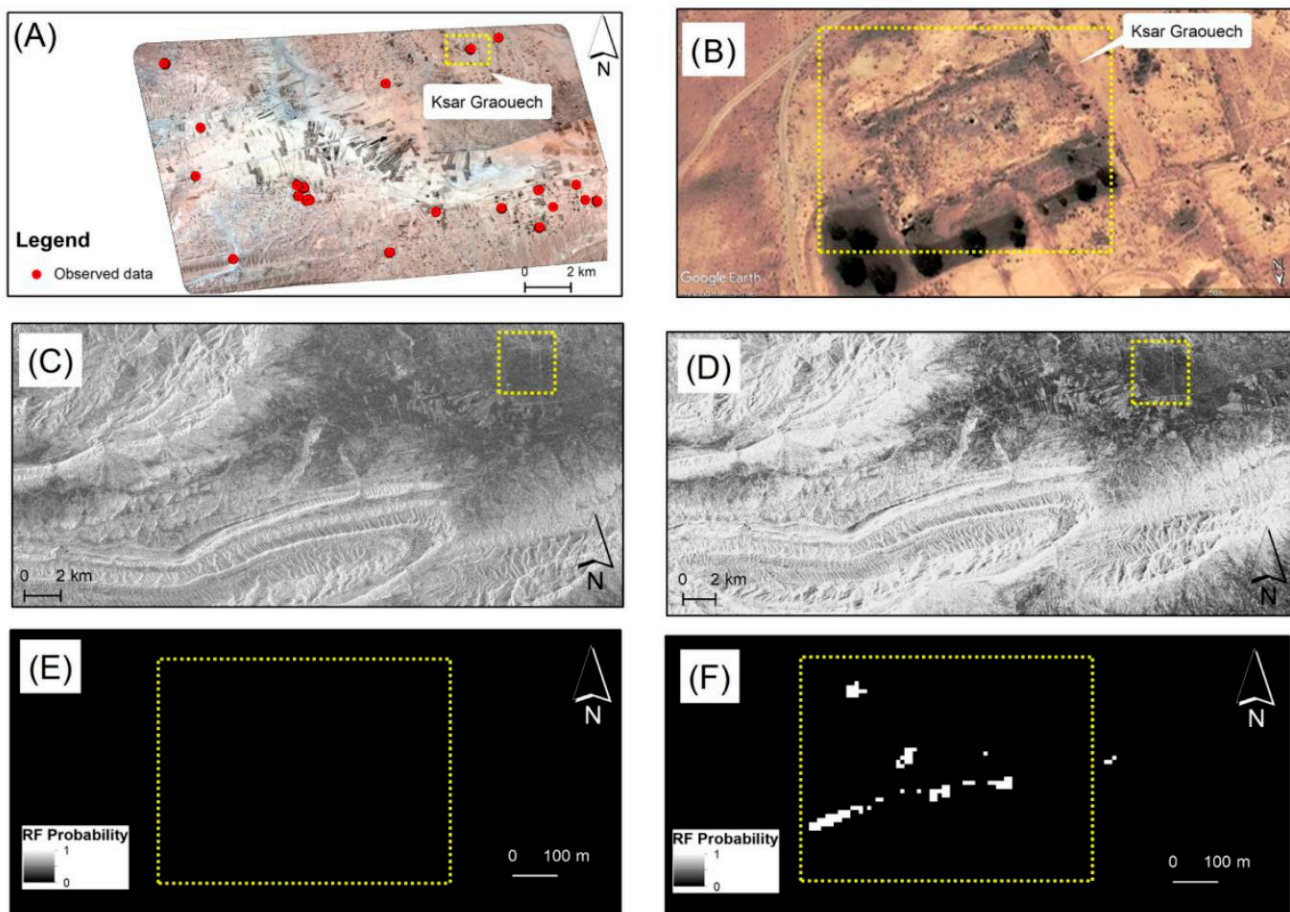


Figure 4. (A) The study area, showing the distribution of sites. (B) A Google Earth base map locating a well-preserved fort. (C) Dual Sentinel-1 band [VV, VH] in ascending mode. (D) Single Sentinel-1 band [VV] in ascending mode. Results of the RF classifier: (E) Visible high-resolution PB1 imagery without SAR images compared to the virtual absence of sites. (F) An example of SAR images combined with PB1 that detected a known fortified site used as a validation set; note that the white dots scattered through the region indicate high-RF probability sites.

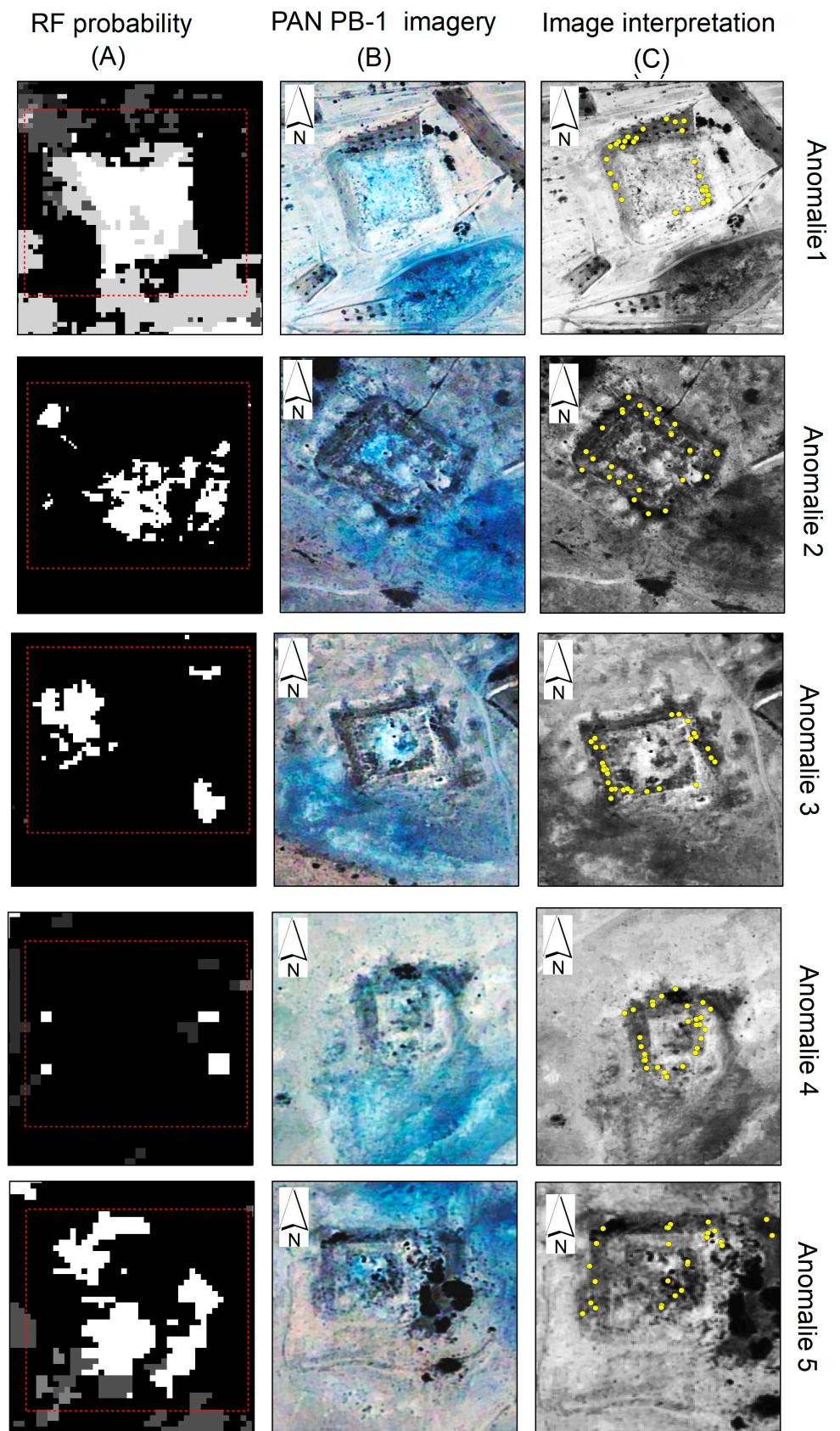


Figure 5. RF probability results. (A) Illustration of fortified detection sites. (B) Clustering of high-probability pixels in the area showing the detection structures of fortified sites. (C) Pan sharpened Pleiades imagery. Image was interpreted as signifying the existence of a fort hidden underground.

4. Discussion

The RF method, which has been used in the classification of remote sensing data since the early 2000s, was chosen as the classification algorithmic rule for this study due to its simplicity of implementation, robustness, and possible predictability [63,68,69]. The challenge we faced was the discovery of fortified sites. Our objective was to develop a straightforward yet efficient methodology that combined remote sensing techniques and automated archaeological remains discovery, as well as to evaluate the potential offered by the combined use of remote sensing data and machine learning to discover fortified sites in arid areas. Using a substantive approach, we confirmed an advantage similar to that of other applications of machine learning techniques, and we show that the RF potential field-detected sites may be considered ancient settlements. In this research, given the high likelihood of improvement in the classification accuracy, we assessed the RF's performance in a wider context (different archaeological features or sites). As shown in the results section, the performance of the RF classifier is highly satisfactory, with a kappa coefficient of 0.91 and a precision and overall accuracy of 0.93 in the "fortified site group." The RF potential area highlights five unknown locations shown on historical maps. The sites are partly hidden by sand, and the RF potential only shows different parts of the structures' fortified sites, which was verified by a field survey. The discovery of these sites is very important because it documents the existence of ancient Roman fortifications. Based on previous studies, there are more sites of Roman civilisation in this area [8,47], and only some small sites have been uncovered by remote sensing methods. Currently, new sites could be included with those previously identified and dated by Bachagha et al. [8,47,67]. To try to understand the changes in the settlement distribution over time, research in southern Tunisia documented all sites encountered, including those of the Roman era. Considering that most of the previously reported sites were settlements attributed to periods of Roman civilisation, there is a high possibility that most of the newly discovered sites were also occupied during the same period. Fortified structures such as fortresses and defensive works are fairly common features of the archaeological landscape in southern Tunisia. Such features have previously been uncovered in the city of Gafsa. In this study, we were able to locate five fortified sites situated south of the Blad Talh area. The fortified sites were built on approximately level ground in a nearly square form that is covered by sand dunes. The layout showed visible signs of erosion on all sides, and loot pits were visible, especially on the south side. Based on our findings in the literature, we propose a suitable reconstruction of the ancient settlement in Gafsa, indicating that the fortifications in the locale were a defence project planned to defend, protect, and control the Limes [8,70–74]. We found fortified sites located in the same area and close to each other, in contrast to previous research [8]. The fortified sites were separated by a distance of approximately 2.5 km. From the machine learning and P1B data of the study area, a red-dashed line rectangle can be seen in Figure 5. Using machine learning and P1B data surveying, we demonstrate the detection of hidden fortified sites in Gafsa, which is well-situated across the frontier of the Roman or Byzantine era in southern Tunisia.

Surveys: Validation and Archaeological Site Significance

Building on recent advances in digital image analysis and feature detection, we developed an RF algorithm that allows the automated detection of these types of enclosures in Pleiades images with high resolution and Sentinel-1 for better archaeological detection. We also used SAR images to increase the accuracy of classification, which provided good results. In addition, we only used the Google Earth Engine for the view, so we cannot use it for building a machine learning detection model. We successfully used the RF model to detect new sites in satellite imagery. The model detected these sites, which we verified and confirmed in the field. We built the training dataset using both Pleiades and Sentinel-1 images in the Google Earth Engine. Of course, the identification of any object or location as archaeological remains based on images requires confirmation from the ground. The discovered sites described above were confirmed in the area of Blad Talh in southern

Tunisia by machine learning, remote sensing data, and field investigation. Other than the surrounding wall and the ruins of the fortified sites, no other archaeological ruins were seen above ground. Almost all the visual features in the analysed RF results were determined to be micro-topographical results of archaeological importance. As a result, our approach reveals a different layout of archaeological sites, and the algorithms identified structures in the area very well. In November 2021, the exploration team arrived at sites approximately 10 km north of the suspected location of the ancient Roman fortification, KSAR GRAOUECH (a square-shaped mark). Each side of the suspected location was measured to be around 50 m long. These anomalies have no intact walls, but the remains of some wall piers were investigated to identify anomalies. Shards of ancient ceramics were scattered among the walls, and their environs date back to the Roman period, as shown in Figure 6G,I,N,L. Buried walls at these five fortified sites were also unearthed, representing the appearance of concealed remains, as shown in Figure 6C,F,H,J,M. The field investigation conducted in this region reveals the existence of a farm dating back between the Roman Empire and Byzantine times based on the discovery of tiles and shards of ancient ceramics from the Roman period. These fortified sites are situated between Capsa (Gafsa) and the coastal towns of Iunci and Lariscus. Controlling one of the passes to the north would have been of obvious strategic importance during the Roman era, a consideration that strongly supports their inclusion in the list of official fortifications of that period. In addition, these sites have common topographical and archaeological features, and their dimensions are relatively similar to each other. According to Trouset [74], these fortified sites are widely spread in the rear Limes area and are located on the immediate edge of a Roman road or in a control location of a passage; some have been identified as military works that are a part of the defensive system. In the report by Rebuffat et al. [75], these were probably fortified farms that adopted a plan inspired by the military project. The parallels between military architecture and these fortified sites, namely Mattingly Qsur, are very evident in the adoption of the rectangular form with towers projecting from two or four facades [76]. The results of studies investigating this type of site in Fazzan and Cyrenaica in eastern and western Libya, respectively, confirm that the peak occupation of fortified sites occurred after the end of the third century and continued in some regions in later times. More specifically, the majority were occupied between the 4th and 6th centuries (350–540 AD) [77].

Indeed, the general landscape of the Blad Talh was a highly important part of the ancient Roman period. As a result, based on our fortified sites and the literature, we firmly conclude that Blad Talh has played a critical historical role in migration between ancient cities located in current-day north and south Tunisia, as attested by the caravan roads. It was also a part of the sensitive defence system (Limes) located along the desert border, as attested by the several forts that protected the area (Figure 7).



Figure 6. Magnified views of anomalies 1 to 5. (A,B) Landscape of the study area. (G,I,N,L) Shards of ancient ceramics. (E) Ancient Architecture element (K) Lintel photographed at the entrance to a fortress. (C,D,F,H,J,M) Field photos of wall remains.

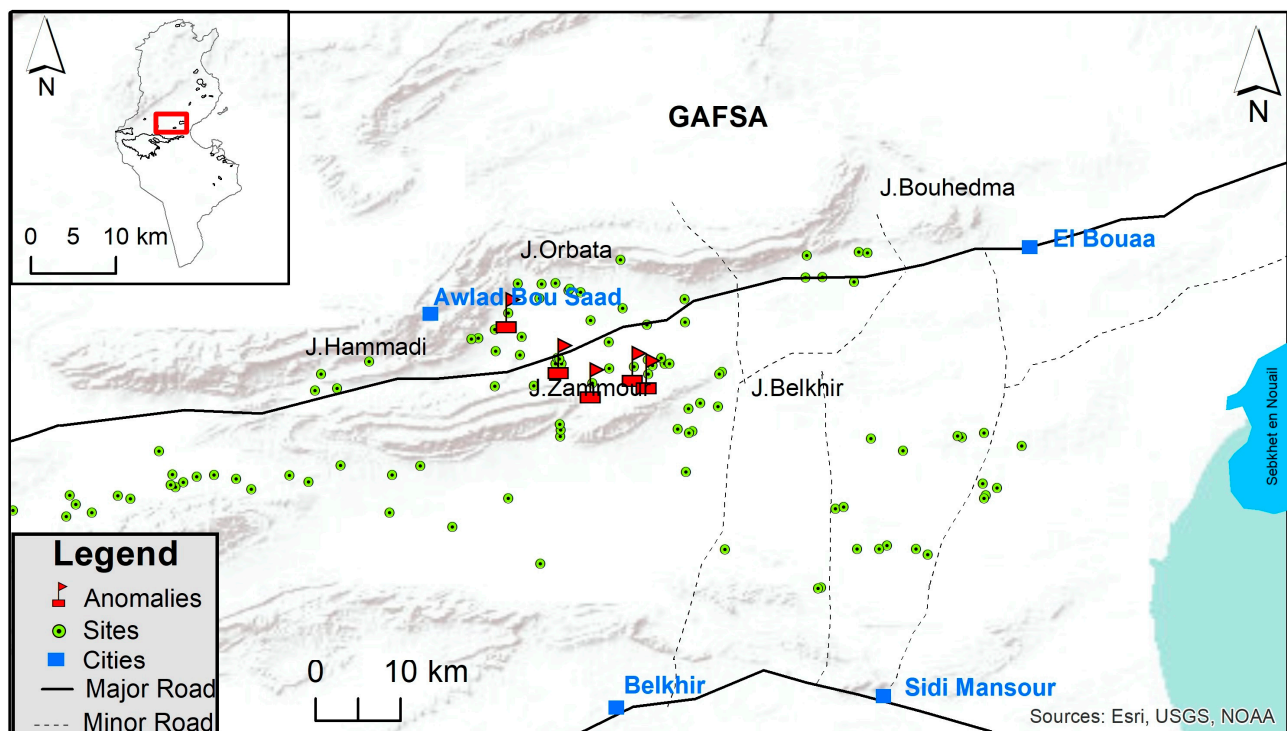


Figure 7. Comprehensive archaeological map of the Blad Talh landscape in the ancient Roman period: localities and ancient road networks. Modified from [71].

5. Conclusions

In summary, we present an integrated workflow that combines SAR images and optical Pleiades imagery with basic spatial analysis in the Google Earth Engine for automatically detecting fortified sites. The random forest-based approach demonstrates that it is a useful tool for overcoming problems with data size and structure. Our research illustrates the applicability of this detection technique to fortifications and demonstrates that it is possible to automate fortification discoveries for the first time in Tunisia. It is possible to summarise insights and knowledge directly from the data, and the algorithm is able to highlight relationships between archaeological sites. The machine-learning algorithm we use is capable of identifying all the currently known sites in the study area and the accurate locations of new fortified sites. The approach provides outputs that are significantly superior to those obtained with a single-source RS technique. RS-based applications in arid and semi-arid regions elsewhere can benefit from the integration of globally available Pleiades and Sentinel data into an accessible, flexible, and repeatable GEE environment to perform and evaluate machine learning workflows. Even though the approach shows accurate results, the limited availability of VHR data and the expense to obtain the data are considered a limitation of this study that can be improved in the future. Archaeological data, along with landscape analysis and mapping items affecting site visibility, indicates that these are only a few of the fortified sites in the region, many of which may be covered by sand in the surveyed area. We discovered fortified sites hidden by thick vegetation and confirmed these sites using field investigation, remote sensing, and machine learning. The outcome of the work presented here provides advances in the technology and archaeology domains. Technologically, using these methods, various derived models are used to evaluate their abilities in investigating the micro-topography of a site of archaeological importance under a sand dune. The results viewed from an archaeological perspective are interesting. The machine learning-based method enabled us to detect five fortified sites for which only some data was obtainable from past records and shed new light on the fortified KSAR GROUECH structure dating back to the Byzantine period (6th century), for which only the presence of a fort was well-known. The findings are validated by on-site

processing, demonstrating that the automatic procedure can identify and extract the major distinctive characteristics of Roman settlements, such as villas and tower walls. Notably, the exploration elaborated in this research is promising in terms of technological invention. By providing for previous quantitative examinations in this region, our exploration raises awareness of the need to use quantitative styles to address more pressing questions, similar to those about the protection and preservation of threatened archaeological sites. As a result, one of the benefits of this research is that it demonstrates, from the perspective of archaeologists, the capability of satellite data and machine learning to discover buried archaeological sites. While this study focuses on archaeological sites in southern Tunisia, the proposed approach is effective in terms of time and cost, particularly in locations where data availability is scarce. Validation of this approach was proved using the nature and characteristics of the study area, and we expect that the classification accuracy of our approach would be further improved by using a convolutional neural network (CNN) and images obtained by the Google Earth Engine.

Author Contributions: Conceptualisation: N.B., W.X. and A.E.; methodology, A.E. and N.B.; software, N.B. and A.E.; validation, N.B., W.X. and A.E.; formal analysis, N.B., W.X. and A.E.; investigation, N.B., M.T. and A.E.; resources, W.X., N.B., and M.T.; data curation, N.B., M.T., A.E., F.S.; writing—original draft preparation, N.B., W.X., A.E., M.T., W.X. and F.S.; writing and supervision, W.X. All authors have read and agreed to the published version of the manuscript.

Funding: This work was supported by the National Natural Science Foundation of China (No. 42174023).

Institutional Review Board Statement: Not applicable.

Informed Consent Statement: Not applicable.

Data Availability Statement: Sentinel-1 data are available via the European Space Agency's Copernicus Open Access Hub <https://scihub.copernicus.eu/> (accessed on 13 July 2021).

Conflicts of Interest: The authors have no conflict of interest to declare.

References

- Giardino, M.; Haley, B.S. Airborne Remote Sensing and Geospatial Analysis. In *Remote Sensing in Archaeology: An Explicitly North American Perspective*; University of Alabama Press: Tuscaloosa, AL, USA, 2006; pp. 47–77.
- Chase, A.F.; Chase, D.Z.; Fisher, C.T.; Leisz, S.J.; Weishampel, J.F. Geospatial revolution and remote sensing LiDAR in Mesoamerican archaeology. *Proc. Natl. Acad. Sci. USA* **2012**, *109*, 12916–12921. [[CrossRef](#)] [[PubMed](#)]
- Lasaponara, R.; Masini, N. Image Enhancement, Feature Extraction and Geospatial Analysis in an Archaeological Perspective. In *Satellite Remote Sensing*; Springer: Berlin/Heidelberg, Germany, 2012; pp. 17–63.
- Leisz, S.J. An Overview of the Application of Remote Sensing to Archaeology during the Twentieth Century. In *Mapping Archaeological Landscapes from Space*; Springer: New York, NY, USA, 2013; pp. 11–19.
- Luo, L.; Wang, X.; Guo, H.; Lasaponara, R.; Zong, X.; Masini, N.; Wang, G.; Shi, P.; Khatteli, H.; Chen, F.; et al. Airborne and spaceborne remote sensing for archaeological and cultural heritage applications: A review of the century (1907–2017). *Remote Sens. Environ.* **2019**, *232*, 111280. [[CrossRef](#)]
- Verhoeven, G.J. Are we there yet? A review and assessment of archaeological passive airborne optical imaging approaches in the light of landscape archaeology. *Geosciences* **2017**, *7*, 86. [[CrossRef](#)]
- Verschoof-van der Vaart, W.B.; Lambers, K. Applying automated object detection in archaeological practice: A case study from the southern Netherlands. *Archaeol. Prospect.* **2022**, *29*, 15–31. [[CrossRef](#)]
- Bachagha, N.; Wang, X.; Luo, L.; Li, L.; Khatteli, H.; Lasaponara, R. Remote sensing and GIS techniques for reconstructing the military fort system on the Roman boundary (Tunisian section) and identifying archaeological sites. *Remote Sens. Environ.* **2020**, *236*, 111418. [[CrossRef](#)]
- Beck, A.; Philip, G.; Abdulkarim, M.; Donoghue, D. Evaluation of Corona and Ikonos high resolution satellite imagery for archaeological prospection in western Syria. *Antiquity* **2007**, *81*, 161–175. [[CrossRef](#)]
- Orengo, H.; Krahtopoulou, A.; Garcia-Molsosa, A.; Palaiochoritis, K.; Stamati, A. Photogrammetric re-discovery of the hidden long-term landscapes of western Thessaly, central Greece. *J. Archaeol. Sci.* **2015**, *64*, 100–109. [[CrossRef](#)]
- Parcak, S. Satellite remote sensing methods for monitoring archaeological tells in the Middle East. *J. Field Archaeol.* **2007**, *32*, 65–81. [[CrossRef](#)]
- Masini, N.; Lasaponara, R. Sensing the Past from Space: Approaches to Site Detection. In *Sensing the Past*; Springer: Berlin/Heidelberg, Germany, 2017; pp. 23–60.

13. Barceló, J.A.; De Almeida, V. Functional analysis from visual and non-visual data. an artificial intelligence approach. *Mediterr. Archaeol. Archaeom.* **2012**, *12*, 273–321.
14. Hatzopoulos, J.N.; Stefanakis, D.; Georgopoulos, A.; Tapinaki, S.; Pantelis, V.; Liritzis, I. Use of Various Surveying Technologies to 3d Digital Mapping and Modelling of Cultural Heritage Structures for Maintenance and Restoration Purposes: The Tholos in Delphi, Greece. *Mediterr. Archaeol. Archaeom.* **2017**, *17*, 311–336.
15. Kaimaris, D. Ancient theaters in Greece and the contribution of geoinformatics to their macroscopic constructional features. *Sci. Cult.* **2018**, *4*, 9–25.
16. Kaimaris, D. Utilization of Different Sensors in Uav for The Detection and Optimal Visual Observation of the Marks over Buried Ancient Remains. *Sci. Cult.* **2022**, *8*, 129–146.
17. Popović, S.; Bulić, D.; Matijašić, R.; Gerometta, K.; Boschian, G. Roman Land Division in Istria, Croatia: Historiography, Lidar, Structural Survey and Excavations. *Mediterr. Archaeol. Archaeom.* **2021**, *21*, 165–178.
18. Fonte, J.; Parcero-Oubiña, C.; Costa-García, J. A GIS-Based Analysis of the Rationale behind Roman Roads. In *The Case of the So-Called via XVII (NW Iberian Peninsula)*; Mediterranean Archaeology and Archaeometry: Mytilene, Greece, 2017; Volume 17, pp. 163–189.
19. Orengo, H.A.; Conesa, F.C.; Garcia-Molsosa, A.; Lobo, A.; Green, A.S.; Madella, M.; Petrie, C.A. Automated detection of archaeological mounds using machine-learning classification of multisensor and multitemporal satellite data. *Proc. Natl. Acad. Sci. USA* **2020**, *117*, 18240–18250. [[CrossRef](#)] [[PubMed](#)]
20. Guyot, A.; Hubert-Moy, L.; Lorho, T. Detecting Neolithic burial mounds from LiDAR-derived elevation data using a multi-scale approach and machine learning techniques. *Remote Sens.* **2018**, *10*, 225. [[CrossRef](#)]
21. Martins, K.; Blenkinsopp, C.E.; Power, H.E.; Bruder, B.; Puleo, J.A.; Bergsma, E.W.J. High-resolution monitoring of wave transformation in the surf zone using a LiDAR scanner array. *Coast. Eng.* **2017**, *128*, 37–43. [[CrossRef](#)]
22. Evans, D.; Fletcher, R. The landscape of Angkor Wat redefined. *Antiquity* **2015**, *89*, 1402–1419. [[CrossRef](#)]
23. Biagetti, S.; Merlo, S.; Adam, E.; Lobo, A.; Conesa, F.C.; Knight, J.; Bekrani, H.; Crema, E.R.; Alcaina-Mateos, J.; Madella, M. High and medium resolution satellite imagery to evaluate late Holocene human–environment interactions in arid lands: A case study from the Central Sahara. *Remote Sens.* **2017**, *9*, 351. [[CrossRef](#)]
24. Thabeng, O.L.; Merlo, S.; Adam, E. High-resolution remote sensing and advanced classification techniques for the prospection of archaeological sites’ markers: The case of dung deposits in the Shashi-Limpopo Confluence area (southern Africa). *J. Archaeol. Sci.* **2019**, *102*, 48–60. [[CrossRef](#)]
25. Cigna, F.; Tapete, D.; Lasaponara, R.; Masini, N. Amplitude change detection with ENVISAT ASAR to image the cultural landscape of the Nasca region, Peru. *Archaeol. Prospect.* **2013**, *20*, 117–131. [[CrossRef](#)]
26. Assaf, A.T.; Sayl, K.N.; Adham, A. Surface Water Detection Method for Water Resources Management. *J. Phys. Conf. Ser.* **2021**, *1973*, 012149. [[CrossRef](#)]
27. Muneer, A.S.; Sayl, K.N.; Kamal, A.H. Modeling of spatially distributed infiltration in the Iraqi Western Desert. *Appl. Geomat.* **2021**, *13*, 467–479. [[CrossRef](#)]
28. Agapiou, A.; Lysandrou, V.; Hadjimitsis, D.G. Optical remote sensing potentials for looting detection. *Geosciences* **2017**, *7*, 98. [[CrossRef](#)]
29. Cigna, F.; Tapete, D. Tracking human-induced landscape disturbance at the nasca lines UNESCO world heritage site in Peru with COSMO-SkyMed InSAR. *Remote Sens.* **2018**, *10*, 572. [[CrossRef](#)]
30. Tapete, D.; Cigna, F.; Donoghue, D. ‘Looting marks’ in space-borne SAR imagery: Measuring rates of archaeological looting in Apamea (Syria) with TerraSAR-X Staring Spotlight. *Remote Sens. Environ.* **2016**, *178*, 42–58. [[CrossRef](#)]
31. Bennett, R.; Cowley, D.; De Laet, V. The data explosion: Tackling the taboo of automatic feature recognition in airborne survey data. *Antiquity* **2014**, *88*, 896–905. [[CrossRef](#)]
32. Davis, D.S. Object-based image analysis: A review of developments and future directions of automated feature detection in landscape archaeology. *Archaeol. Prospect.* **2019**, *26*, 155–163. [[CrossRef](#)]
33. LiDAR, A.M.D.U. Object-Based Image Analysis in Beaufort County, SC. *Southeast. Archaeol.* **2019**, *38*, 23–37.
34. Trier, D.; Cowley, D.; Waldeland, A.U. Using deep neural networks on airborne laser scanning data: Results from a case study of semi-automatic mapping of archaeological topography on Arran, Scotland. *Archaeol. Prospect.* **2019**, *26*, 165–175. [[CrossRef](#)]
35. Gorelick, N.; Hancher, M.; Dixon, M.; Ilyushchenko, S.; Thau, D.; Moore, R. Google Earth Engine: Planetary-scale geospatial analysis for everyone. *Remote Sens. Environ.* **2017**, *202*, 18–27. [[CrossRef](#)]
36. Gualandi, M.L.; Gattiglia, G.; Anichini, F. An open system for collection and automatic recognition of pottery through neural network algorithms. *Heritage* **2021**, *4*, 140–159. [[CrossRef](#)]
37. Sayl, K.N.; Sulaiman, S.O.; Kamel, A.H.; Muhammad, N.S.; Abdullah, J.; Al-Ansari, N. Minimizing the impacts of desertification in an arid region: A case study of the west desert of Iraq. *Adv. Civ. Eng.* **2021**, *2021*, 5580286. [[CrossRef](#)]
38. Caspari, G.; Crespo, P. Convolutional neural networks for archaeological site detection—Finding “princely” tombs. *J. Archaeol. Sci.* **2019**, *110*, 104998. [[CrossRef](#)]
39. Chen, L.; Priebe, C.E.; Sussman, D.L.; Comer, D.C.; Megarry, W.P.; Tilton, J.C. Enhanced archaeological predictive modelling in space archaeology. *arXiv* **2013**, arXiv:1301.2738.
40. Garcia-Molsosa, A.; Orengo, H.A.; Lawrence, D.; Philip, G.; Hopper, K.; Petrie, C.A. Potential of deep learning segmentation for the extraction of archaeological features from historical map series. *Archaeol. Prospect.* **2021**, *28*, 187–199. [[CrossRef](#)] [[PubMed](#)]

41. Lasaponara, R.; Masini, N. Identification of archaeological buried remains based on the normalized difference vegetation index (NDVI) from Quickbird satellite data. *IEEE Geosci. Remote Sens. Lett.* **2006**, *3*, 325–328. [[CrossRef](#)]
42. Duporge, I.; Isupova, O.; Reece, S.; Macdonald, D.W.; Wang, T. Using very-high-resolution satellite imagery and deep learning to detect and count African elephants in heterogeneous landscapes. *Remote Sens. Ecol. Conserv.* **2021**, *7*, 369–381. [[CrossRef](#)]
43. Fiorucci, M.; Khoroshiltseva, M.; Pontil, M.; Traviglia, A.; Del Bue, A.; James, S. Machine learning for cultural heritage: A survey. *Pattern Recognit. Lett.* **2020**, *133*, 102–108. [[CrossRef](#)]
44. Yaworsky, P.M.; Vernon, K.B.; Spangler, J.D.; Brewer, S.C.; Coddling, B.F. Advancing predictive modeling in archaeology: An evaluation of regression and machine learning methods on the Grand Staircase-Escalante National Monument. *PLoS ONE* **2020**, *15*, e0239424. [[CrossRef](#)]
45. Akinosho, T.D.; Oyedele, L.O.; Bilal, M.; Ajayi, A.O.; Delgado, M.D.; Akinade, O.O.; Ahmed, A.A. Deep learning in the construction industry: A review of present status and future innovations. *J. Build. Eng.* **2020**, *32*, 101827. [[CrossRef](#)]
46. Khanoussi, M. Note sur la date de promotion de Capsa (Gafsa, en Tunisie) au rang de colonie romaine (Note d'information). *Comptes Rendus Séances L'académie Inscr. Belles-Lett.* **2010**, *154*, 1009–1020. [[CrossRef](#)]
47. Bachagha, N.; Xu, W.; Luo, X.; Masini, N.; Brahmi, M.; Wang, X.; Souei, F.; Lasaponara, R. On the Discovery of a Roman Fortified Site in Gafsa, Southern Tunisia, Based on High-Resolution X-Band Satellite Radar Data. *Remote Sens.* **2022**, *14*, 2128. [[CrossRef](#)]
48. Tissot, C. Géographie comparée de la province romaine d'Afrique, 261. *Paris* **1884**, *8*, 160.
49. Euzennat, M. Quatre années de recherches sur la frontière romaine en Tunisie méridionale. *Comptes Rendus Séances L'académie Inscr. Belles-Lett.* **1972**, *116*, 7–27. [[CrossRef](#)]
50. Toussaint, P.-M.; Guéneau, L.L.J. Résumé des Reconnaissances Archéologiques Exécutées par les Officiers des Brigades Topographiques d'Algérie et de Tunisie Pendant la Campagne 1903-1904», in BCTH. pp. 223–241. Available online: https://scholar.google.com/scholar?hl=en&as_sdt=0%2C5&q=PM+Toussaint%2C+LLJ+Gu%2C%A9neau+-+1904&btnG= (accessed on 19 January 2023).
51. Stewart, C.; Oren, E.D.; Cohen-Sasson, E. Satellite remote sensing analysis of the Qasrawet archaeological site in North Sinai. *Remote Sens.* **2018**, *10*, 1090. [[CrossRef](#)]
52. D'Andrimont, R.; Lemoine, G.; van der Velde, M. Targeted grassland monitoring at parcel level using sentinels, street-level images and field observations. *Remote Sens.* **2018**, *10*, 1300. [[CrossRef](#)]
53. D'Andrimont, R.; Verhegghen, A.; Lemoine, G.; Kempeneers, P.; Meroni, M.; van der Velde, M. From parcel to continental scale—A first European crop type map based on Sentinel-1 and LUCAS Copernicus in-situ observations. *Remote Sens. Environ.* **2021**, *266*, 112708. [[CrossRef](#)]
54. Lee, J.-S. Refined filtering of image noise using local statistics. *Comput. Graph. Image Process.* **1981**, *15*, 380–389. [[CrossRef](#)]
55. Elnashar, A.; Zeng, H.; Wu, B.; Fenta, A.A.; Nabil, M.; Duerler, R. Soil erosion assessment in the Blue Nile Basin driven by a novel RUSLE-GEE framework. *Sci. Total Environ.* **2021**, *793*, 148466. [[CrossRef](#)]
56. Zeng, H.; Elnashar, A.; Wu, B.; Zhang, M.; Zhu, W.; Tian, F.; Ma, Z. A framework for separating natural and anthropogenic contributions to evapotranspiration of human-managed land covers in watersheds based on machine learning. *Sci. Total Environ.* **2022**, *823*, 153726. [[CrossRef](#)]
57. Elnashar, A.; Zeng, H.; Wu, B.; Gebremicael, T.G.; Marie, K. Assessment of environmentally sensitive areas to desertification in the Blue Nile Basin driven by the MEDALUS-GEE framework. *Sci. Total Environ.* **2022**, *815*, 152925. [[CrossRef](#)] [[PubMed](#)]
58. Carneiro, T.; Da Nobrega, R.V.M.; Nepomuceno, T.; Bian, G.-B.; De Albuquerque, V.H.C.; Filho, P.P.R. Performance analysis of google colabouratory as a tool for accelerating deep learning applications. *IEEE Access* **2018**, *6*, 61677–61685. [[CrossRef](#)]
59. Guyot, A.; Lennon, M.; Lorho, T.; Hubert-Moy, L. Combined detection and segmentation of archeological structures from LiDAR data using a deep learning approach. *J. Comput. Appl. Archaeol.* **2021**, *4*, 1. [[CrossRef](#)]
60. Kamel, A.H.; Afan, H.A.; Sherif, M.; Ahmed, A.N.; El-Shafie, A. RBFNN versus GRNN modeling approach for sub-surface evaporation rate prediction in arid region. *Sustain. Comput. Inform. Syst.* **2021**, *30*, 100514. [[CrossRef](#)]
61. Soroush, M.; Mehrtash, A.; Khazraee, E.; Ur, J.A. Deep learning in archaeological remote sensing: Automated qanat detection in the Kurdistan region of Iraq. *Remote Sens.* **2020**, *12*, 500. [[CrossRef](#)]
62. Yang, S.; Luo, L.; Li, Q.; Chen, Y.; Wu, L.; Wang, X. Auto-identification of linear archaeological traces of the Great Wall in northwest China using improved DeepLabv3+ from very high-resolution aerial imagery. *Int. J. Appl. Earth Obs. Geoinf.* **2022**, *113*, 102995. [[CrossRef](#)]
63. Breiman, L. Random forests. *Mach. Learn.* **2001**, *45*, 5–32. [[CrossRef](#)]
64. Kheir, A.M.; Ammar, K.A.; Amer, A.; Ali, M.G.; Ding, Z.; Elnashar, A. Machine learning-based cloud computing improved wheat yield simulation in arid regions. *Comput. Electron. Agric.* **2022**, *203*, 107457. [[CrossRef](#)]
65. Breiman, L. Bagging predictors. *Mach. Learn.* **1996**, *24*, 123–140. [[CrossRef](#)]
66. Tuvdendorj, B.; Zeng, H.; Wu, B.; Elnashar, A.; Zhang, M.; Tian, F.; Nabil, M.; Nanzad, L.; Bulkhbai, A.; Natsagdorj, N. Performance and the Optimal Integration of Sentinel-1/2 Time-Series Features for Crop Classification in Northern Mongolia. *Remote Sens.* **2022**, *14*, 1830. [[CrossRef](#)]
67. Bachagha, N.; Luo, L.; Wang, X.; Masini, N.; Moussa, T.; Khatteli, H.; Lasaponara, R. Mapping the Roman water supply system of the Wadi el Melah Valley in Gafsa, Tunisia, using remote sensing. *Sustainability* **2020**, *12*, 567. [[CrossRef](#)]

68. Gislason, P.O.; Benediktsson, J.A.; Sveinsson, J.R. Random Forest Classification of Multisource Remote Sensing and Geographic Data. In Proceedings of the IGARSS 2004. 2004 IEEE International Geoscience and Remote Sensing Symposium, Anchorage, AK, USA, 20–24 September 2004; IEEE: Piscataway, NJ, USA, 2004.
69. Feng, Q.; Liu, J.; Gong, J. UAV remote sensing for urban vegetation mapping using random forest and texture analysis. *Remote Sens.* **2015**, *7*, 1074–1094. [[CrossRef](#)]
70. Moussa, T. Essai D'identification d'un Oronyme de l'Antiquité Tardive: L'Agalumnus de la Johannide. In *Africa et in Moesia: Borders of the Roman World Sharing Heritage of North Africa and the Lower Danube*; Bucharest University Press and National Commission of Romania for UNESCO: Paris, France, 2021; pp. 107–116.
71. Moussa, T. Bled Talh (Sudtunisien) dans l'Antiquité: l'occupation du Sol. In *Thèse de Doctorat en Histoire Ancienne. (Dir. Abellatif Mrabet)*; FLSH: Sousse, Tunisie, 2020; 365p.
72. Pringle, D. The Defence of Byzantine Africa, from Justinian to the Arab Conquest. In *An Account of the Military History and Archaeology of the African Provinces the Sixth and Seventh Centuries*; International Series; BAR: Oxford, UK, 1981; p. 99.
73. Mrabet, A. Identité de la Tripolitaine Occidentale: De Quelques Signalements Archéologiques. In *Provinces et Identités Provinciales Dans l'Afrique Romaine*; Tables rondes du CRAHM: Caen, France, 2011; pp. 221–237.
74. Troussat, P. *Recherches sur le Limes Tripolitanus du Chott El-Djérid à la Frontière Tuniso-Libyenne*; CNRS: Paris, France, 1974; p. 135.
75. Rebuffat, C.F.R. Les Fermiers du désert Dans L'Africaromana V. In Proceedings of the Attidel V Convegno di Studio, Sassari, Italy, 11–13 December 1988; pp. 35–43.
76. Mattingly, D.J.; Sterry, M.; Leitch, V. Fortified Farms and Defended Villages of Late Roman and Late Antique Africa. 2013. Available online: https://scholar.google.com/scholar?hl=en&as_sdt=0%2C5&q=77.Emrage%2C+A.S.+Roman+Fortified+Farms+%28qsur%29+and+Military+Sites+in+the+Region+of+the+Wadi+Al-Kuf%2C+Cyrenaica+%28Eastern+Libya%29.+Ph.D.+Dissertation%2C+University+of+Leicester%2C+Leicester%2C+UK%2C+2015.&btnG= (accessed on 19 January 2023).
77. Emrage, A.S. Roman Fortified Farms (qsur) and Military Sites in the Region of the Wadi Al-Kuf, Cyrenaica (Eastern Libya). Ph.D. Dissertation, University of Leicester, Leicester, UK, 2015.

Disclaimer/Publisher's Note: The statements, opinions and data contained in all publications are solely those of the individual author(s) and contributor(s) and not of MDPI and/or the editor(s). MDPI and/or the editor(s) disclaim responsibility for any injury to people or property resulting from any ideas, methods, instructions or products referred to in the content.